acylation of the amino group of daunosamine (3) results in the formation of a binary complex involving only the drug and Cu(II).

References

Arcamone, F., Cassinelli, G., Fantini, G., Grein, A., Orezzi, P., Pol, C., & Spalla, C. (1969) *Biotechnol. Bioeng. 11*, 1101.

Bachur, N. R. (1979) *Cancer Treat. Rep. 63*, 817.

Barthelemy-Clavey, V., Maurizot, J. C., & Sicara, P. J. (1973) *Biochimie 55*, 859.

Calendi, E., DiMarco, A., Reggiani, M., Scarpinato, B., & Valentini, L. (1965) *Biochim. Biophys. Acta 103*, 25.

Carter, S. K. (1980) *Drugs 20*, 375.

DiMarco, A., & Arcamone, F. (1975) *Arzneim.-Forsch. 25*, 368.

DiMarco, A., Gaetani, M., Orezzi, P., Scarpinato, B., Silvertrini, R., Soldati, M., Dasdia, M., & Valentini, L. (1964) *Nature (London) 201*, 706.

Eichhorn, G. L. (1973) *Inorg. Biochem. 2*, 1191.

Eichhorn, G. L., & Clark, P. (1965) *Proc. Natl. Acad. Sci. U.S.A. 47*, 778.

Fishman, M. M., & Schwartz, I. (1974) *Biochem. Pharmacol. 23*, 2147.

Förster, W., Bauer, E., Schütz, H., Berg, H., Akimenko, M., Minchenkova, L. E., Eudokimov, Yu. M., & Warshavsky, Ya. M. (1979) *Biopolymers 18*, 625.

Gabbay, E. J., Grier, D., Fingerle, R. E., Reimer, R., Levy, R., Pearle, S. W., & Wilson, W. D. (1976) *Biochemistry 15*, 2062.

Greenaway, F. T., & Dabrowiak, J. C. (1982) *J. Inorg. Biochem. 16*, 91.

Lown, J. W., Sim, S.-K., Majumdar, K. C., & Chang, R.-Y. (1977) *Biochem. Biophys. Res. Commun. 76*, 705.

Martin, S. R. (1980) *Biopolymers 19*, 713.

Mikelens, P., & Levinson, W. (1978) *Bioinorg. Chem. 9*, 441.

Patel, D. J., & Canuel, L. L. (1978) *Eur. J. Biochem. 90*, 247.

Pigram, W. J., Fuller, W., & Hamilton, L. D. (1972) *Nature (London) 235*, 17.

Quigley, G. J., Wang, A. H., Ughetto, G., Van Der Marcel, G., Van Boom, J. H., & Rich, A. (1980) *Proc. Natl. Acad. Sci. U.S.A. 77*, 7204.

Rifkind, J. M., Shin, Y. A., Heim, J. M., & Eichhorn, G. L. (1976) *Biopolymers 15*, 1879.

Rusconi, A. (1966) *Biochim. Biophys. Acta 123*, 627.

Someya, A., & Tanaka, N. (1979) *J. Antibiot. 32*, 839.

Underwood, A. L., Toribara, T. Y., & Newman, W. F. (1950) *J. Am. Chem. Soc. 72*, 5597.

Zimmer, C. H., Luck, G., Fritzsche, H., & Triebel, H. (1971) *Biopolymers 10*, 441.

Zunino, F., DiMarco, A., Zaccara, A., & Gambetta, R. A. (1980) *Biochim. Biophys. Acta 607*, 206.

Synthesis and Properties of ApU Analogues Containing 2′-Halo-2′-deoxyadenosines. Effects of 2′ Substituents on Oligonucleotide Conformation†

Seiichi Uesugi, Toshinori Kaneyasu, and Morio Ikehara*

ABSTRACT: Five A-U analogues containing deoxyadenosine or 2′-halo-2′-deoxyadenosines, which are known to have widely different C3′-endo conformer populations according to their electronegativities of the halogen substituents, dAfl-U, dAcl-U, dAbr-U, dAio-U, and dA-U, were synthesized chemically. Characterization of these dimers has been performed by UV absorption, circular dichroism, and proton nuclear magnetic resonance spectroscopy. The results show that the dimers containing 2′-halo-2′-deoxyadenosines have stacked conformations with a geometry similar to that of A-U and the degree of stacking decreases in the order dAfl-U > dAcl-U > dAbr-U > dAio-U. dAcl-U is assumed to have the same degree of stacking as A-U. dA-U takes a more stacked conformation than does dAio-U, but the mode of stacking is different from those of the other dimers. The effects of the 2′ substituents on dimer conformation are discussed in terms of electronegativity, molecular size, and hydrophobicity.

DNA and RNA have different structures as well as different functions. The difference in chemical structures resides in α substituents at C2′ (H for DNA and OH for RNA). It is known that DNA usually takes a B-form structure and that RNA only takes an A-form structure from X-ray diffraction analysis of nucleic acid fibers (Arnott, 1970). Recently, these conclusions were confirmed by X-ray analysis of crystals of a double-helical dodecadeoxyribonucleotide (Drew et al., 1981) and a tRNA [e.g., Quigley et al. (1975)]. One of the major conformational differences in the monomer units of DNA and RNA, which produces differences in polymer conformation as a whole, is the difference in sugar puckering (C2′ endo for B-form DNA and C3′ endo for RNA). It is known that the furanose ring conformation of nucleoside derivatives in solution can be described as an equilibrium between C3′-endo and C2′-endo forms (Altona & Sundaralingam, 1973; Evans & Sarma, 1974). Recently, it was shown from ^{1}H NMR[1] studies

† From the Faculty of Pharmaceutical Sciences, Osaka University, Suita, Osaka 565, Japan. *Received May 27, 1982.* This research was supported in part by a Grant-in-Aid for Scientific Research from the Ministry of Education, Science and Culture of Japan. This is paper 64 in the series Polynucleotides. For paper 63, see Uesugi et al. (1981b).

[1] Abbreviations: dAfl, 2′-fluoro-2′-deoxyadenosine; dAcl, 2′-chloro-2′-deoxyadenosine; dAbr, 2′-bromo-2′-deoxyadenosine; dAio, 2′-iodo-2′-deoxyadenosine; NMR, nuclear magnetic resonance; CD, circular dichroism; UV, ultraviolet; TLC, thin-layer chromatography; DSS, sodium 3-(trimethylsilyl)propane-1-sulfonate; MS, mass spectrum; MeOTr, monomethoxytrityl; Bz, benzoyl; DMF, dimethylformamide; TEAB, triethylammonium bicarbonate; DCC, dicyclohexylcarbodiimide; DEAE, diethylaminoethyl; other abbreviations principally follow the recommendation of the IUPAC–IUB Commission on Biochemical Nomenclature (1970, 1977).

0006-2960/82/0421-5870$01.25/0

of 2′-substituted 2′-deoxynucleoside derivatives that the population of the C3′-endo form increases with electronegativity of the 2′ substituent (Uesugi et al., 1979; Guschlbauer & Jankowski, 1980). These findings explain why ribonucleoside derivatives generally have a higher population of the C3′-endo form than do deoxyribonucleoside derivatives at the monomer level (Davies & Danyluk, 1974; Lee et al., 1976; Cheng & Sarma, 1977). Among adenine nucleosides, the 2′-fluoro derivative shows the largest C3′-endo population (65%), and the 2′-iodo derivative shows the lowest (7%). Those of adenosine and deoxyadenosine are 36% and 19%, respectively (Uesugi et al., 1979). The effects of 2′ substituents on oligonucleotide conformation were the next subject to be studied. We have examined A-A analogues containing 2′-fluoro-2′-deoxyadenosine (dAfl) and showed that these dimers take more stable stacked conformations than does A-A (Uesugi et al., 1981a). It was assumed that the highly polar nature of the C2′-F bond and the extreme preference for C3′-endo puckering may stabilize the stacked conformation in an A-form structure. This idea is supported by the fact that poly(dAfl) is an efficient template for viral reverse transcriptase (De Clercq et al., 1979) and a messenger for in vitro protein synthesis (Fukui et al., 1982). Moreover, poly(dIfl)·poly(C) can induce interferon as effectively as poly(I)·poly(C) in several cell lines (De Clercq et al., 1980).

In this paper, we report the synthesis and properties of four A-U analogues containing 2′-halo-2′-deoxyadenosines, dAfl-U (**3a**), dAcl-U (**3b**), dAbr-U (**3c**), dAio-U (**3d**), and dA-U (**3e**), and discuss the effects of the 2- substituents on oligonucleotide stacking. The 2′-halo-2′-deoxyadenosines (dAx) have a wide variety of average sugar puckering conformations. The A-U analogues contain different bases and sugars, and therefore, their ^{1}H NMR signals can be easily assigned. Moreover, there is the possibility that they can form self-duplexes.

Materials and Methods

General Procedures. Paper chromatography was performed by a descending technique on Whatman No. 1 paper with the following solvent systems: solvent A, 1-butanol–acetic acid–water (5:2:3); solvent B, ethanol–1 M ammonium acetate (pH 7.0)(7:3); solvent C, 2-propanol–concentrated NH_4OH–water (7:1:2); solvent D, saturated $(NH_4)_2SO_4$–water–2-propanol (79:19:2). Paper electrophoresis (PEP) was performed for 1 h with a voltage gradient of 35 V/cm on Toyo filter paper No.51A with the following buffer systems: buffer A, 0.05 M triethylammonium bicarbonate (TEAB) (pH 7.5); buffer B, 0.2 M morpholinium acetate (pH 3.5); buffer C, 0.05 M sodium borate (pH 9.2). Thin-layer chromatography (TLC) was performed on Merck silica gel $60F_{254}$ with $CHCl_3$–methanol mixtures. Activated charcoal for chromatography (code no. 031-02135) was supplied by Wako Pure Chemical Industries, Ltd., Osaka, Japan. Nuclease P1 was obtained from Yamasa Shoyu Co., and the incubation was carried out in 0.05 M ammonium acetate (pH 5.0) at 37 °C for 6 h with the enzyme at 20–100 μg/mL.

UV absorption spectra were recorded on a Hitachi 200-10 spectrophotometer. CD spectra were recorded on a JASCO ORD/UV-5 spectropolarimeter equipped with a CD attachment. For temperature variation experiments, a thermojacketed cell and a Neslab RTE-8 circulating bath were used. The temperature of the cell was measured with a Shibaura MGB-III thermister. The molar absorption coefficient, ϵ, and the molar ellipticity, $[\theta]$, are presented in terms of per base residue values. ^{1}H NMR spectra were recorded with a Hitachi R-900 spectrometer (90 MHz) operating in the Fourier-transform mode. Each dimer sample was passed through columns of Dowex 50 (Na^+ form) and then Chelex 100 resins and lyophilized 3 times from D_2O solution after adjusting the pH. The dimers and monomers (both about 12 mM) were measured at pD 7.5 and 5.5, respectively. The ^{1}H NMR chemical shifts were determined relative to internal *tert*-butyl alcohol, which had in turn been referenced to DSS (sodium 3-(trimethylsilyl)propane-1-sulfonate). Mass spectra (MS) were recorded with a JEOL JMS-D300 spectrometer.

2′-Halo-2′-deoxyadenosines were synthesized by a modified procedure of Ikehara & Miki (1978). 2′-Chloro-2′-deoxyadenosine 3′-phosphate was synthesized by condensation of 5′-*O*-(monomethoxytrityl)-N^6-benzoyl-2′-chloro-2′-deoxyadenosine and 2-cyanoethyl phosphate with DCC (A. Ohta, unpublished results). Phosphorus analysis was carried out by a combination of the methods of Baginski et al. (1967) and Chen et al. (1956).

5′-O-(Monomethoxytrityl)-N^6-benzoyl-2′-fluoro-2′-deoxyadenosine (**1a**). Benzoyl chloride (0.42 mL) was added dropwise to a stirred solution of dAfl (215 mg, 0.8 mmol) in pyridine at 0 °C. The mixture was stirred at room temperature for 1 h. Water (1 mL) was added, and the mixture was stirred at room temperature for 30 min. The solvent was evaporated and water added. The mixture was extracted with $CHCl_3$, and the combined extracts were dried over anhydrous $MgSO_4$. After removal of solvent, a solution of the residue in pyridine (3 mL)–ethanol (3 mL) was treated with 2 N NaOH (2.5 mL) at room temperature for 15 min. Pyridinium Dowex 50 resin (10 mL) was added to neutralize the solution. The whole mixture was poured into a column, and the resin was washed with aqueous pyridine (50%). The combined eluants were evaporated to dryness. The residue was dried by evaporation with pyridine and treated with monomethoxytrityl chloride (225 mg) in DMF (3 mL)–benzene (3 mL)–pyridine (0.5 mL) at room temperature for 2 h with stirring. After removal of solvents, water was added to the residue, and the mixture was extracted with $CHCl_3$. The combined extracts were dried over anhydrous $MgSO_4$ and evaporated to dryness. A solution of the residue in $CHCl_3$ was added dropwise to *n*-hexane. The precipitates were collected by centrifugation and dried over P_2O_5. The yield of **1a** was 260 mg (40%): MS, *m/e* (70 eV) 372 (M^+ – MeOTr), 273 ($MeOTr^+$). This compound gave a positive color test for the trityl group.

5′-O-(Monomethoxytrityl)-N^6-acetyl-2′-chloro-2′-deoxyadenosine (**1b**). dAcl (155 mg, 0.54 mmol) was treated with acetic anhydride (1.1 mL) in pyridine (2.7 mL) at 80 °C for 3 h. After evaporation of volatile materials, the residue was evaporated with toluene–ethanol (1:1). A solution of the residue in ethanol (4.9 mL) was treated with 2 N NaOH (3.5 mL) at 0 °C for 3 min with stirring. Pyridinium Dowex 50 resin (10 mL) was added, and the mixture was filtered. The resin was washed with aqueous pyridine (50%). The filtrate and washing were combined and evaporated to dryness. The residue was dried by evaporation with pyridine and then treated with monomethoxytrityl chloride (330 mg) in pyridine (2.2 mL) at room temperature for 5 h with stirring. After removal of the solvent, the residue was worked up as described for **1a**. The yield of **1b** was 263 mg (0.44 mmol, 81%): UV λ_{max}^{EtOH} 233 nm, 272.5 nm; MS, *m/e* 601 ($M^+ + 1$), 599 ($M^+ - 1$).

5′-O-(Monomethoxytrityl)-N^6-acetyl-2′-bromo-2′-deoxyadenosine (**1c**). N^6-Acetyl-2′-bromo-2′-deoxyadenosine was prepared as described above for **1b** starting from dAbr (165 mg, 0.5 mmol) and treated with monomethoxytrityl chloride (310 mg) in pyridine (2 mL)–DMF (1 mL) at room temperature for 5 h. Workup as above gave 263 mg of **1c** (0.41

mmol, 82%): UV λ_{max}^{EtOH} 233 nm, 272.5 nm; MS, *m/e* 645 ($M^+ + 1$), 643 ($M^+ - 1$).

5'-O-(Monomethoxytrityl)-N⁶-acetyl-2'-iodo-2'-deoxyadenosine (**1d**). dAio (165 mg, 0.44 mmol) was treated as described for **1c**. The yield of **1d** was 288 mg (0.42 mmol, 95%): UV λ_{max}^{EtOH} 233 nm, 272.5 nm; MS, *m/e* 691 (M^+).

5'-O-(Monomethoxytrityl)-N⁶-acetyl-2'-deoxyadenosine (**1e**). Deoxyadenosine (150 mg, 0.6 mmol) was treated as described for **1b**. Tritylation was carried out with monomethoxytrityl chloride (280 mg) in pyridine (5 mL) at room temperature for 7 h. The yield of **1e** was 273 mg (0.48 mmol, 80%). This compound was homogeneous on TLC and positive in the color test for trityl group.

2',3'-Di-O-acetyluridine 5'-Phosphate (**2**). The sodium salt of uridine 5'-phosphate (184 mg, 0.5 mmol) was converted to the pyridinium salt on a column of pyridinium Dowex 50 resin. The pyridinium salt was dried by evaporation with pyridine and treated with acetic anhydride (0.8 mL) in pyridine (3.5 mL) at room temperature for 4 h with stirring. After removal of solvent, the residue was treated with aqueous pyridine (50%, 5 mL) at room temperature for 1 h. After removal of solvent, the residue was dried by evaporation with pyridine, **2** was precipitated with ether (80 mL) from its solution in a small volume of pyridine. The yield was 197 mg (0.4 mmol, 80%), PEP(C) R_m(pU-U) 0.52.

2'-Bromo-2'-deoxyadenosine 3'-Phosphate (**4**). A mixture of **1c** (163 mg, 0.25 mmol) and pyridinium 2-cyanoethyl phosphate, which was prepared from the barium salt (100 mg, 0.35 mmol), was dried by evaporation with pyridine. The residue was treated with DCC (417 mg, 2 mmol) in pyridine (1.3 mL) at 30 °C for 60 h. Concentrated NH_4OH (20 mL) was added, and the mixture was kept at 55 °C for 2 h. After removal of volatile materials, the residue was treated with acetic acid (12 mL)–water (3 mL) at room temperature for 3 h with stirring. The solid material was filtered off, and the filtrate was evaporated to dryness. $CHCl_3$ was added, and the mixture was extracted with water containing 5% pyridine. After a washing with $CHCl_3$, the aqueous extracts were evaporated to dryness. The residue was dissolved in 0.01 N HCl (100 mL) and applied on a column of charcoal for chromatography (8 mL). The column was thoroughly washed with water then eluted with ethanol–water–concentrated NH_4OH (50:45:5). The eluant was evaporated. An aqueous solution of the residue was applied on a column (1.4 × 11 cm) of Dowex 1-X2 (formate form). Elution was carried out with a linear gradient of formic acid (0–0.15 M, total 2 L). A total of 2540 A_{260} units of **4** (68%) was eluted at around 0.12 M formic acid concentration. The chromatographic properties are presented in Table I. The ^1H NMR data are shown in Table III.

2'-Iodo-2'-deoxyadenosine 3'-Phosphate (**5**). Phosphorylation of **1d** (140 mg, 0.2 mmol) was performed as described above. After a desalting with a charcoal column, **5** was isolated by chromatography on a column (1.2 × 7 cm) of Dowex 1-X2 (formate form) resin. Elution was carried out with a linear gradient of formic acid (0–0.2 M, total 2 L). A total of 920 A_{260} units of **5** (33%) was eluted at around 0.14 M formic acid concentration. The chromatographic properties are presented in Table I. The ^1H NMR data are shown in Table III.

dAfl-U (**3a**). A mixture of **1a** (206 mg, 0.36 mmol) and **2** (197 mg, 0.4 mmol) was treated with DCC (825 mg, 4 mmol) in pyridine (3 mL) at 30 °C for 60 h. Water (0.5 mL) was added, and the mixture was kept at room temperature for 10 h. The dicyclohexylurea was filtered off, and the filtrate was evaporated to dryness. A solution of the residue in methanol (10 mL) was saturated with ammonia at 0 °C and then kept at room temperature for 10 h. After removal of volatile materials, the residue was treated with acetic acid (8 mL)–water (2 mL) at room temperature for 3 h. TLC in $CHCl_3$–ethanol (4:1) showed complete disappearance of the tritylated dimer at the origin. The solvent was evaporated, and $CHCl_3$ and water were added. The dimer was extracted with water. The combined aqueous extracts were washed with $CHCl_3$ and evaporated to dryness. An aqueous solution (200 mL) of the residue was applied on a column (1.2 × 38 cm) of DEAD-cellulose (bicarbonate form). Elution was carried out with a linear gradient of triethylammonium bicarbonate (TEAB) buffer (pH 7.5, 0–0.2 M, total 3 L). The fractions containing **3a** (5760 A_{260} units, 76%) were combined and desalted by repeated coevaporation with water. **3a** was further purified by chromatography on a column (1.2 × 22 cm) of Dowex 1-X2 (formate form) with a linear gradient of formic acid (0–0.30 M, total 2 L). A total of 4020 A_{259} units of **3a** (54%) was eluted at around 0.18 M formic acid concentration. Formic acid was removed by coevaporation with water and lyophilization. The chromatographic properties and UV and ^1H NMR data are presented in Tables I–III. The CD spectra are shown in Figures 2 and 7.

dAcl-U (**3b**). A mixture of **1b** (260 mg, 0.43 mmol) and **2** (210 mg, 0.43 mmol) was treated with DCC (660 mg, 3.2 mmol) in pyridine (3.5 mL) at 30 °C for 70 h. After removal of the solvent, the residue was treated with concentrated NH_4OH (10 mL)–ethanol (10 mL) at room temperature for 10 h. After removal of volatile materials, the residue was treated with acetic acid (16 mL)–water (4 mL) at room temperature for 3 h with stirring. The disappearance of the tritylated compound at the origin was monitored by TLC in $CHCl_3$–ethanol (4:1). Solid materials were filtered off, and the filtrate was evaporated to dryness. The residue was worked up as described above for **3a**. Chromatography on a column (1.8 × 34 cm) of DEAE-cellulose (bicarbonate form) with a linear gradient of TEAB buffer (0–0.20 M, total 3 L) gave 3500 A_{260} units of **3b** (37%). Further purification by chromatography on a column (1.2 × 12.5 cm) of Dowex 1-X2 (formate form) with a linear gradient of formic acid (0–0.30 M, total 2 L) gave 2050 A_{259} units of **3b** (22%), which was eluted at around 0.18 M formic acid concentration. The chromatographic properties and UV and ^1H NMR data are presented in Tables I–III. The CD spectra are shown in Figures 3 and 8.

dAbr-U (**3c**). A mixture of **1c** (260 mg, 0.4 mmol) and **2** (300 mg, 0.62 mmol) was treated with DCC (660 mg, 3.2 mmol) in pyridine (3.2 mL) at 30 °C for 74 h. The reaction mixture was worked up as described for **3b**. Acyl groups were removed with concentrated NH_4OH (5 mL)–ethanol (5 mL). The monomethoxytrityl group was removed with acetic acid (6.4 mL)–water (1.6 mL). Chromatography on a column (1.8 × 36 cm) of DEAE-cellulose gave 7200 A_{260} units of **3c** (78%). Further purification on a column (1.2 × 13 cm) of Dowex 1-X2 resin gave 5230 A_{259} units of **3c** (57%), which was eluted at around 0.18 M formic acid concentration. The chromatographic properties and UV and ^1H NMR data are presented in Tables I–III. The CD spectra are shown in Figures 4 and 9.

dAio-U (**3d**). A mixture of **1d** (285 mg, 0.41 mmol) and **2** (245 mg, 0.5 mmol) was treated with DCC (682 mg, 3.3 mmol) in pyridine (2.3 mL) at 30 °C for 80 h. The reaction mixture was worked up as described for **3c**. Chromatography on a column (1.8 × 40 cm) of DEAE-cellulose gave 6530 A_{260} units of **3d** (70%). Further purification on a column (1.2 ×

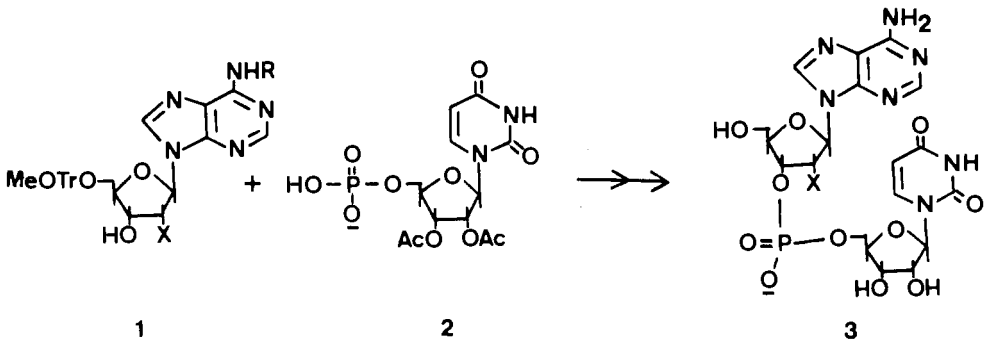

FIGURE 1: Synthetic scheme for dinucleoside monophosphates.

Table I: Chromatographic Properties of Dinucleoside Monophosphates

compound	PEP[a] R_m(pA-A)[b] in buffer A	PEP[a] R_m(pA-A)[b] in buffer B	PC[a] R_f in solvent A	PC[a] R_f in solvent B	PC[a] R_f in solvent C	PC[a] R_f in solvent D
dAfl-U	0.57	1.13	0.20	0.39	0.36	0.12
dAcl-U	0.54	1.09	0.26	0.42	0.42	0.08
dAbr-U	0.54	1.07	0.31	0.43	0.43	0.07
dAio-U	0.50	1.03	0.33	0.43	0.43	0.05
dA-U	0.55	1.05	0.17	0.38	0.34	0.10
pA	1.00	1.00	0.23	0.18	0.27	0.25
pU			0.16	0.19	0.16	0.75
A	0.00	0.00	0.55	0.58	0.54	0.16
U		0.45	0.45	0.66	0.46	0.66

[a] Compositions of buffer for paper electrophoresis (PEP) and solvent systems for paper chromatography (PC) are given under Materials and Methods. [b] Relative mobility to pA (1.0) and adenosine (0.0).

13 cm) of Dowex 1-X2 resin gave 4820 A_{259} units of **3d** (52%), which was eluted at around 0.18 M formic acid concentration. The chromatographic properties and UV and ^{1}H NMR data are presented in Tables I–III. The CD spectra are shown in Figures 5 and 10.

dA-U (**3e**). A mixture of **1e** (270 mg, 0.47 mmol) and **2** (372 mg, 0.76 mmol) was treated with DCC (970 mg, 4.7 mmol) at 30 °C for 70 h. The reaction mixture was worked up as described for **3c**. Chromatography on a column (1.8 × 42 cm) of DEAE-cellulose gave 2670 A_{260} units of **3e** (25%), which was eluted at around 0.05 M TEAB concentration. The chromatographic properties and UV and ^{1}H NMR data are shown in Tables I–III. The CD spectra are shown in Figures 6 and 11.

Results

Synthesis of Dinucleoside Monophosphates. The synthetic scheme for the dimers (**3a–3d**) is shown in Figure 1. A deoxyadenosine derivative with a free 3′-OH (**1**) and 2′,3′-di-*O*-acetyluridine 5′-phosphate (**2**) were condensed with dicyclohexylcarbodiimide (DCC) in pyridine at room temperature for 60–80 h. The amino group of the adenine moiety was protected to avoid possible side reactions as observed in the case of A-A analogues (Uesugi et al., 1981a). For protection of the amino group, a benzoyl group was used for **1a** and later an acetyl group for **1b–1d** because of the simpler workup. After condensation and deprotection, the dimer was isolated by DEAE-cellulose column chromatography. The dimer was further purified by chromatography on Dowex 1 resin. All these dimers could be completely hydrolyzed with snake venom phosphodiesterase or nuclease P1 (Fujimoto et al., 1974) to give the corresponding nucleoside and nucleoside 5′-phosphate in a 1:1 ratio. Chromatographic properties (Table I), UV spectra (Table II), phosphorus analysis (Table II), CD spectra (Figures 2–11), and ^{1}H NMR spectra (Table III) all support the assigned dimer structures.

Table II: Ultraviolet Absorption Data of Dinucleoside Monophosphates

compound	pH	λ_{max} (nm)	λ_{min} (nm)	ϵ(P) at λ_{max}[a]	hypochromicity (%)[b]
dAfl-U	2	258	231	22 500	
	7	260	231	21 000	12
	12	259	234	19 800	
dAcl-U	2	259	230	22 400	
	7	261	231	21 900	10
	12	260	234	20 700	
dAbr-U	2	259	231	23 900	
	7	261	231	23 000	7.5
	12	260	234	22 800	
dAio-U	2	259	231	22 900	
	7	261	231	22 700	5
	12	260	234	22 600	
dA-U	2	259	231	23 900	
	7	261	230	23 000	8
	12	260	234	21 900	

[a] Determined by phosphorus analysis and given in ϵ per phosphate residue. UV spectra were measured at room temperature (≈20 °C). [b] Calculated from hydrolysis experiment with nuclease P1. UV spectra were measured at room temperature (≈20 °C). Absorbances at λ_{max}'s before and after digestion were compared.

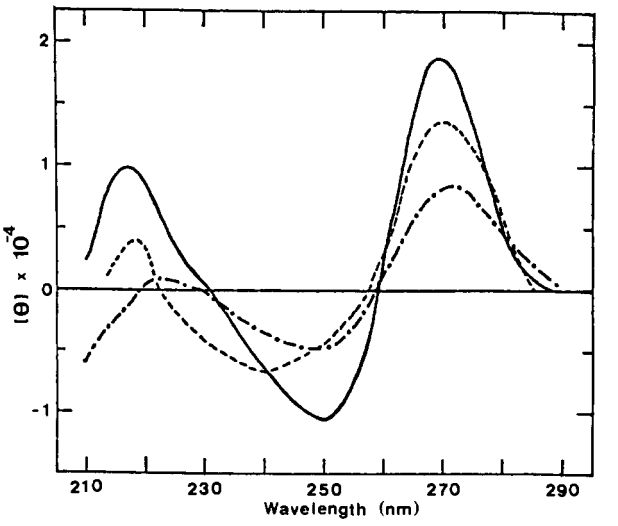

FIGURE 2: CD spectra of dAfl-U in 0.01 N HCl [pH 2 (–·–)], 0.01 M sodium phosphate buffer [pH 7 (—)], and 0.01 N NaOH [pH 12 (---)] containing 0.1 M NaCl at room temperature (≈28 °C).

Ultraviolet Absorption Spectra. All the dimers show similar characteristic changes of UV absorption with pH changes (Table II). At pH 2, a shift of λ_{max} to shorter wavelength and an increase in ϵ_{max} are observed with respect to those of the neutral spectrum. This phenomenon suggests protonation on the adenine residue and subsequent destacking (Johnson & Schleich, 1974). At pH 12, a shift of λ_{min} to longer wavelength

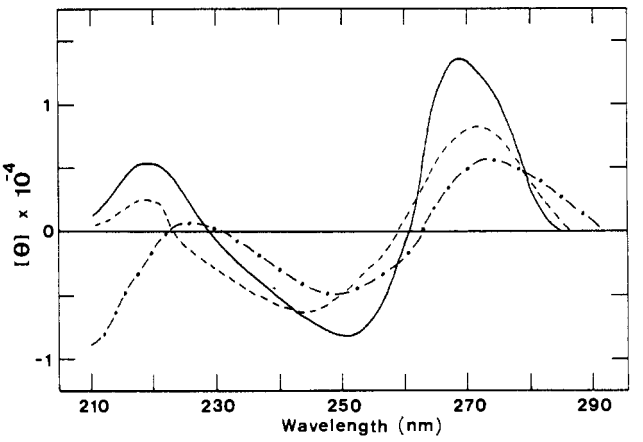

FIGURE 3: CD spectra of dAcl-U in 0.01 N HCl [pH 2 (-·-)], 0.01 M sodium phosphate buffer [pH 7 (—)], and 0.01 N NaOH [pH 12 (---)] containing 0.1 M NaCl at room temperature (≈28 °C).

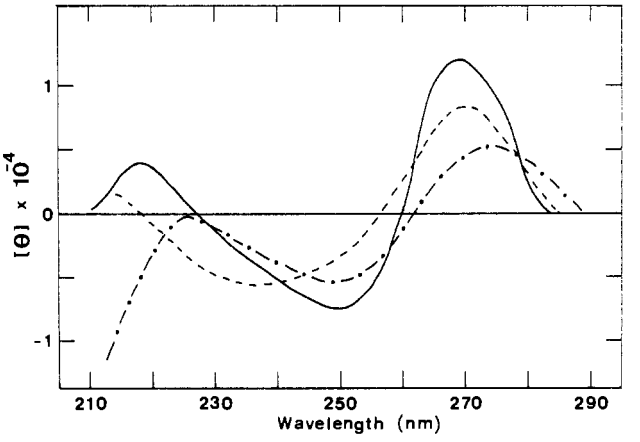

FIGURE 4: CD spectra of dAbr-U in 0.01 N HCl [pH 2 (-·-)], 0.01 M sodium phosphate buffer [pH 7 (—)], and 0.01 N NaOH [pH 12 (---)] containing 0.1 M NaCl at room temperature (≈28 °C).

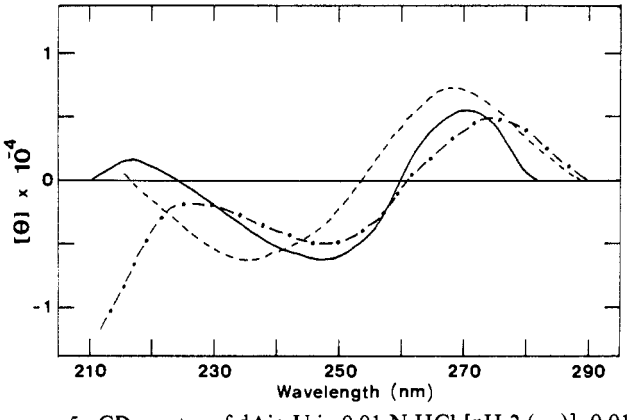

FIGURE 5: CD spectra of dAio-U in 0.01 N HCl [pH 2 (-·)], 0.01 M sodium phosphate buffer [pH 7 (—)], and 0.01 N NaOH [pH 12 (---)] containing 0.1 M NaCl at room temperature (≈28 °C).

and a decrease in ϵ_{max} are observed with respect to those of the neutral spectrum. This reflects proton dissociation in the uracil residues. Concomitant destacking is suggested from the CD spectrum at pH 12 as discussed below. We note that dAfl-U shows a shorter λ_{max} (by 1 nm) and the smallest ϵ_{max} at all three pH's when compared with those of the other dimers. Hypochromicity data (Table II), which were obtained from nuclease P1 digestion experiments, suggest that the degree of stacking decreases in the order dAfl-U > dAcl-U > dA-U ≈ dAbr-U > dAio-U. In the case of the dimers containing halo groups, this order follows the electronegativity

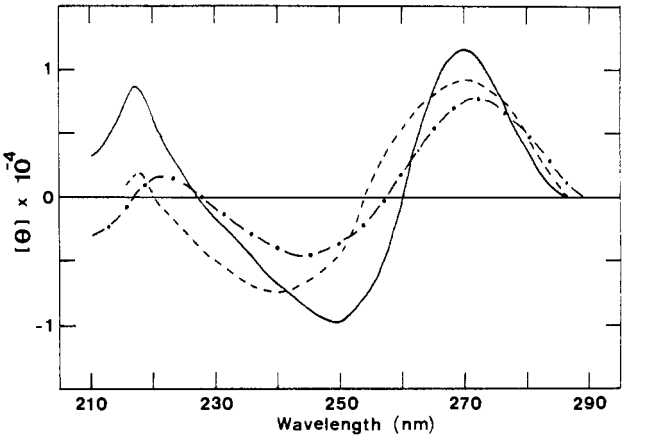

FIGURE 6: CD spectra of dA-U in 0.01 N HCl [pH 2 (-·-)], 0.01 M sodium phosphate buffer [pH 7 (—)], and 0.01 N NaOH [pH 12 (---)] containing 0.1 M NaCl at room temperature (≈28 °C).

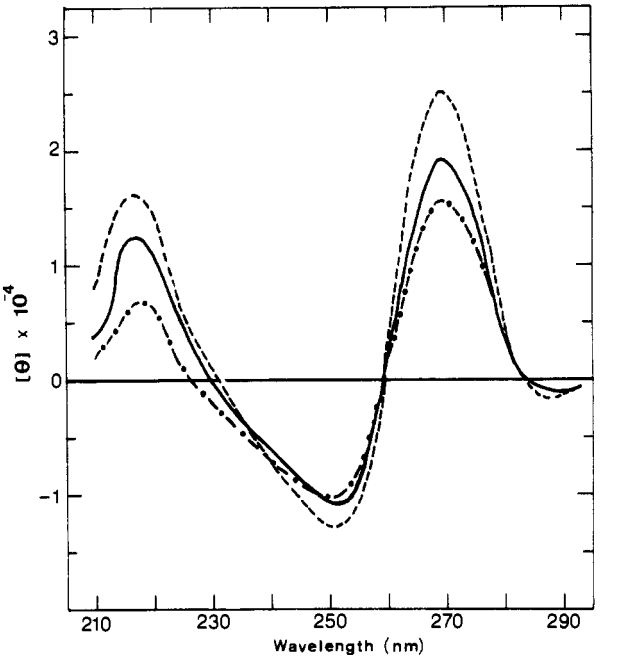

FIGURE 7: CD spectra of dAfl-U in 0.1 M NaCl–0.01 M sodium phosphate buffer (pH 7.0) at 2 (---), 20 (—), and 40 °C (-·-).

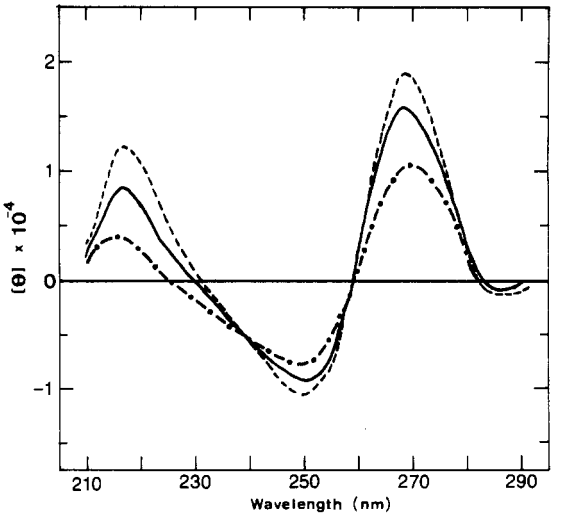

FIGURE 8: CD spectra of dAcl-U in 0.1 M NaCl–0.01 M sodium phosphate buffer (pH 7.0) at 2 (---), 20 (—), and 40 °C (-·-).

of the substituents and also the C3′-endo conformer population of the substituted deoxyadenosines (Uesugi et al., 1979).

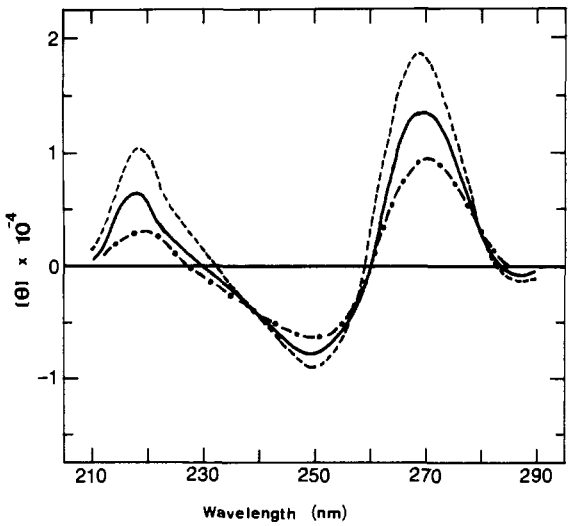

FIGURE 9: CD spectra of dAbr-U in 0.1 M NaCl–0.01 M sodium phosphate buffer (pH 7.0) at 2 (---), 20 (—), and 40 °C (-·-).

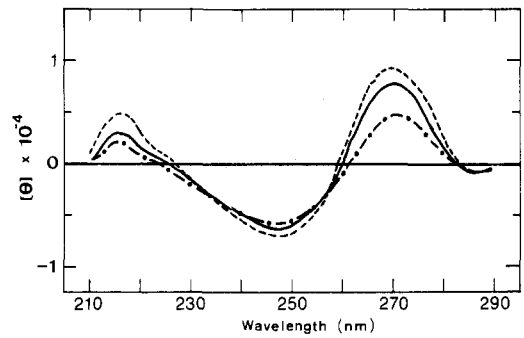

FIGURE 10: CD spectra of dAio-U in 0.1 M NaCl–0.01 M sodium phosphate buffer (pH 7.0) at 2 (---), 20 (—), and 40 °C (-·-).

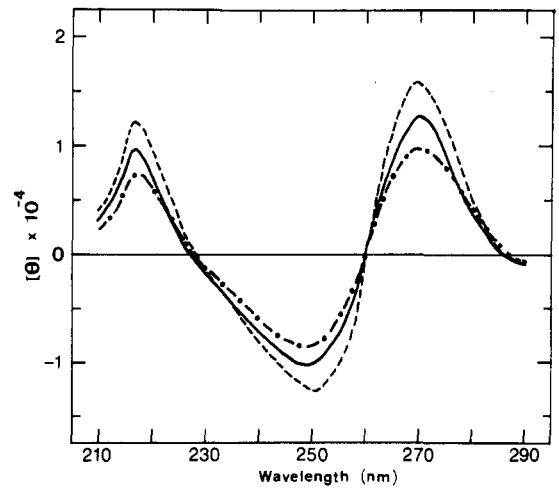

FIGURE 11: CD spectra of dA-U in 0.1 M NaCl–0.01 M sodium phosphate buffer (pH 7.0) at 2 (---), 20 (—), and 40 °C (-·-).

Hypochromicity of A-U is reported to be 10% under similar conditions (Olsthoorn et al., 1980a), which is the same as that of dAcl-U.

Circular Dichroism Spectra. CD spectra of each dimer at three pH's (2, 7, and 12) are shown in Figures 2–6, and the spectra at three temperatures (2, 20, and 40 °C) are shown in Figures 7–11. All the dimers show characteristic changes upon pH variation. At pH 12 and especially at pH 2, the magnitudes of the CD bands generally decrease with respect to those at pH 7. These results suggest that both types of ionization at the base residues cause destacking (Warshaw & Tinoco, 1965). In the case of dAio-U, the magnitudes of CD

Table III: ^{1}H NMR Data of Dinucleoside Monophosphates and Related Compounds[a]

compound		chemical shift (ppm)[b] H8 (H6)	H2 (H5)	H1′	$J_{1',2'}$ (Hz)
dAfl-U	dAflp-	8.33	8.16	6.33	1.5
	-pU	7.67	5.51	5.71	2.9
dAcl-U	dAclp-	8.35	8.17	6.27	4.6
	-pU	7.76	5.65	5.76	2.6
dAbr-U	dAbrp-	8.35	8.18	6.38	5.3
	-pU	7.77	5.69	5.78	2.8
dAio-U	dAiop-	8.33	8.19	6.43	7.1
	-pU	7.83	5.78	5.84	3.1
dA-U	dAp-	8.28	8.18	6.40	6.8
	-pU	7.70	5.64	5.80	3.9
dAflp		8.30	8.15	6.35	2.9
dAclp		8.37	8.23	6.31	6.6
dAbrp		8.37	8.24	6.40	7.1
dAiop		8.35	8.24	6.44	8.7
pU		7.95	5.93	5.96	4.1

[a] Solutions of the dimers and monomers (about 12 mM) in D_2O were measured at 34 °C and at pD 7.5 and 5.5, respectively. [b] Measured downfield from DSS reference.

bands at pH 7 are already small, and the differences are not significant. The dimer spectral patterns at neutral pH, two positive bands at around 215 and 270 nm and a negative band at around 215 nm, are very similar to that of A-U (Warshaw & Cantor, 1970). Therefore, these dimers may take a conformation similar to that of A-U, an anti-anti, right-handed stack. Stability of the stacking to thermal perturbation was examined by temperature-variation experiments. The magnitudes of all three bands of each dimer decrease with increasing temperature. The $[\theta]_{max}$ around 270 nm decreases by 40–50% over the temperature range of 2–40 °C. In the dAx-U series (x = fl, cl, and br) where relatively large CD bands are observed, the $[\theta]_{max}$ change (%) increases in the following order: dAfl-U (36%) < dAcl-U (42%) < dAbr-U (52%). dA-U shows a small $[\theta]_{max}$ change (37%) comparable to that of dAfl-U. Comparison of the CD band magnitudes at 20 °C suggests that the degree of stacking decreases in the following order: dAfl-U > dAcl-U > dAbr-U ≈ dA-U > dAio-U. This order is almost the same as suggested by UV hypochromicity data. The magnitudes for dAbr-U are about the same as those of A-U measured under similar conditions (Warshaw & Cantor, 1970). Careful examination of the CD spectra of dAx-U in the long-wavelength region reveals the existence of very small negative bands at around 285 nm, which are emphasized in Figures 7–10. A similar negative band has been observed for A-U and Am-U in 4.7 M KF (Drake et al., 1974) and also for m^6A-U and m_2^6A-U (Olsthoorn et al., 1980a).

^{1}H Nuclear Magnetic Resonance Spectra. ^{1}H NMR spectra of the dimers and component monomers were measured to obtain detailed information about stacking conformations. The chemical shifts of the base and sugar-1′ protons and coupling constants between H1′ and H2′ ($J_{1',2'}$) are presented in Table III. Signals of the dAxp- and -pU residues in a dimer are easily distinguished because of the different chemical shifts. H5 of a -pU residue can be assigned from its coupling with H6. As to adenine base signals, those at lower field were assigned to H8 of dAxp- residues as generally observed in adenine nucleoside derivatives. This assignment seems reasonable since the neighboring uracil residue only has weak shielding power (Giessner-Prettre & Pullman, 1976). Changes of chemical shifts and coupling constants upon dimerization were calculated as shown in Table IV. The $\Delta\delta$, δ(monomer)

Table IV: Dimerization Effects on Chemical Shifts and Coupling Constants

compound		Δδ (ppm)[a] H8 (H6)	H2 (H5)	H1′	$\Delta J_{1',2'}$ (Hz)[b]
dAfl-U	dAflp-	−0.03	−0.01	0.02	1.4
	-pU	0.28	0.42	0.25	1.2
dAcl-U	dAclp-	0.02	0.06	0.04	2.0
	-pU	0.19	0.28	0.20	1.5
dAbr-U	dAbrp-	0.02	0.06	0.02	1.8
	-pU	0.18	0.24	0.18	1.3
dAio-U	dAiop-	0.02	0.05	0.01	1.6
	-pU	0.12	0.15	0.12	1.0
dA-U	dAp-[c]	0.00	−0.02	0.06	1.4
	-pU	0.25	0.29	0.16	0.2

[a] $\Delta\delta = \delta(\text{monomer}) - \delta(\text{dimer})$. [b] $\Delta J = J(\text{monomer}) - J(\text{dimer})$. [c] The monomer data were taken from Olsthoorn et al. (1980b).

$-\delta$(dimer), represents the degree of shielding of a proton by anisotropic effects of the neighboring base residue (Giessner-Prettre & Pullman, 1976) and, therefore, can give a measure of stacking interactions. All dAx-U's show similar shielding patterns at the uridine protons, the largest $\Delta\delta$ on H5 with comparable $\Delta\delta$'s on H6 and H1′. The magnitude of $\Delta\delta$ for each proton decreases in the following order: dAfl-U > dAcl-U > dAbr-U > dAio-U. A-U is reported to show a similar shielding pattern on the same protons: 0.24 ppm (H6), 0.35 ppm (H5), and 0.25 ppm (H1′) at 20 °C (Ezra et al., 1977). dA-U shows a different shielding pattern. The $\Delta\delta$ of H6 is closer to that of H5, and the $\Delta\delta$ of H1′ is relatively small. The $\Delta\delta$ of H5 is about the same as that for dAcl-U.

As observed at the nucleoside level (Uesugi et al., 1979), the $J_{1',2'}$ of dAxp increases in the following order: dAflp < dAclp < dAbrp < dAiop. This means that the C3′-endo population of dAxp decreases in the same order (Altona & Sundaralingam, 1973), which is the order of 2′-substituent electronegativity. When these residues are incorporated into the dimers, the $J_{1',2'}$'s decrease by about 1.5–2 Hz while the relative order of the $J_{1',2'}$'s remains unchanged. The -pU residues in the dimers also show decreases of $J_{1',2'}$ by 1–1.5 Hz. In the case of dA-U, the dAp- residue is assumed to show a decrease of $J_{1',2'}$ by 1.4 Hz (Olsthoorn et al., 1980b), but the -pU residue shows almost no change in $J_{1',2'}$. This result again suggests that dA-U takes somewhat different conformations to those of dAx-U's. A-U shows the same degree of $J_{1',2'}$ decreases, 2.4 Hz (Ap-) and 1.4 Hz (-pU) at 20 °C (Ezra et al., 1977), as those of dAcl-U.

Discussion

As described above, the results obtained by all three techniques, UV hypochromicity, CD, and ^{1}H NMR, suggest that degree of stacking decreases in the following order: dAfl-U > dAcl-U > dAbr-U > dAio-U. A-U seems to have a stacked conformation as strong as that of dAcl-U because $[\theta]_{max}$ and $\Delta\delta$(H5) approach those of dAcl-U when the temperature factors are taken into account. These comparisons should be valid since ^{1}H NMR data suggest that these dimers have the same mode of stacking [cf. the crystal structure of A-U double helix (Seeman et al., 1976)]. In the case of dA-U, however, such direct comparison may not be valid since stacking is different as judged by the different shielding pattern in ^{1}H NMR. Nevertheless, it seems that dA-U takes a much more strongly stacked conformation than dAio-U.

The series of halo groups differ from each other in two properties, electronegativity and molecular size. The electronegativity increases in the order I (2.68) < Br (2.94) < Cl (3.19) < F (3.93) (Dailey & Shoolery, 1955) and the molecular size (van der Waals radius in angstroms) increases in the reversed order F (1.35) < Cl (1.80) < Br (1.95) < I (2.15) (Corey–Pauling–Koltun molecular models). Corresponding values for OH and H are as follows: electronegativity, 3.51 and 2.20; van der Waals radius (Å), 1.67 (the long axis) and 1.00, respectively. It should be noted that the molecular volume defined by the van der Waals radius (r) is proportional to r^3. Higher electronegativity of a 2′ substituent makes the C2′–X bond more polar. This has two effects, an increased preference for C3′-endo puckering (Uesugi et al., 1979) and an increased capacity for electrostatic interaction, which will be repulsive to the surrounding negatively polarized or charged atoms. The former effect favors stacking of A-form type, and the latter may destabilize stacking of the B-form type, which requires C2′-endo furanose puckering (Uesugi et al., 1981a). The larger molecular size of a 2′ substituent will also destabilize stacking, especially of B-form type, by steric repulsion. Consideration of both electronegativity and molecular size factors suggests that all dAx-U's including A-U will prefer A-form stacking to B form and the degree of stacking will decrease in the order dAfl-U > dAcl-U > dAbr-U > dAio-U. When dAfl-U and A-U are compared, the observed stacking, dAfl-U > A-U, can be explained similarly because the 2′-fluoro group has higher electronegativity and smaller size. However, when dAcl-U and A-U are compared, the result, dAcl-U ≈ A-U, cannot be explained by these factors only since the 2′-chloro group has lower electronegativity and larger size. To explain this result, it may be assumed that the 2′-chloro group has a hydrophobic, attractive interaction with the adjacent sugar residue, presumably with O (1′). This interaction may also enhance the hydrophobicity of the space between the nucleoside residues stabilizing the stacking interaction. The 2′-hydroxyl group, which contains a polar C–O bond as well as a polar O–H bond, is much more hydrophilic. Therefore, it may have weaker hydrophobic interactions and greater hydration. It has been reported by Drake et al. (1974) that 2′-O-methylated dinucleoside monophosphates, Xm-Y, show enhanced stacking with respect to the corresponding unmethylated X-Y when X = G, C, and U, the bases of which have relatively weak stacking power and are prone to hydration. This result can be explained by similar hydrophobic interactions of the methyl groups, which overcome the destabilizing effects of steric hindrance. In the case of dAio-U and dA-U, both iodo and hydrogen groups have low electronegativities. Therefore, reduced stacking in dAio-U must be due to the bulkiness of the substituent. The iodo group should also have the hydrophobic attractive force but may be too large to be accomodated in the space between the stacking nucleoside residues. Conversely, the hydrogen group is so small that it fits into both A-form and B-form conformations. It causes neither electrostatic nor steric repulsions even in the C2′-endo furanose conformation where it takes a pseudoequatorial position.

In conclusion, the present results suggest that a 2′ substituent on the 3′-nucleotidyl unit of a dinucleoside monophosphate exerts at least four effects on the stacking conformation. These are steric repulsion, furanose puckering preference, electrostatic repulsion, and hydrophobic attraction, which are determined by the molecular size, electronegativity, and hydrophobicity of the substituent, respectively. The conformational difference between DNA and RNA can be explained by these effects of H and OH.

Acknowledgments

We thank Dr. Alexander F. Markham for reading the manuscript.

References
Altona, C., & Sundaralingam, M. (1973) *J. Am. Chem. Soc. 95*, 2333–2344.
Arnott, S. (1970) *Prog. Biophys. Mol. Biol. 21*, 267–318.
Baginski, E. S., Foa, P. P., & Zak, B. (1967) *Clin. Chem. (Winston-Salem, N.C.) 13*, 326–332.
Chen, P. S., Jr., Torribara, T. Y., & Warner, H. (1956) *Anal. Chem. 28*, 1756–1758.
Cheng, D. M., & Sarma, R. H. (1977) *J. Am. Chem. Soc. 99*, 7333–7348.
Dailey, B. P., & Shoolery, J. N. (1955) *J. Am. Chem. Soc. 77*, 3977–3981.
Davies, D. B., & Danyluk, S. S. (1974) *Biochemistry 13*, 4417–4434.
De Clercq, E., Fukui, T., Kakiuchi, N., Ikehara, M., Hattori, M., & Pfleiderer, W. (1979) *Cancer Lett. (Shannon, Irel.) 7*, 27–37.
De Clercq, E., Stollar, B. D., Hobbs, J., Fukui, T., Kakiuchi, N., & Ikehara, M. (1980) *Eur. J. Biochem. 107*, 279–288.
Drake, A. F., Mason, S. F., & Trim, A. R. (1974) *J. Mol. Biol. 86*, 727–739.
Drew, H. R., Wing, R. M., Takano, T., Broka, C., Tanaka, S., Itakura, K., & Dickerson, R. E. (1981) *Proc. Natl. Acad. Sci. U.S.A. 78*, 2179–2183.
Evans, F. E., & Sarma, R. H. (1974) *J. Biol. Chem. 249*, 4754–4759.
Ezra, F. S., Lee, C.-H., Kondo, N. S., Danyluk, S. S., & Sarma, R. H. (1977) *Biochemistry 16*, 1977–1987.
Fujimoto, M., Kuninaka, A., & Yoshino, H. (1974) *Agric. Biol. Chem. 38*, 777–783.
Fukui, T., Kakiuchi, N., & Ikehara, M. (1982) *Biochim. Biophys. Acta 697*, 174–177.
Giessner-Prettre, C., & Pullman, B. (1976) *Biochem. Biophys. Res. Commun. 70*, 578–581.
Guschlbauer, W., & Jankowski, K. (1980) *Nucleic Acids Res. 8*, 1421–1433.
Ikehara, M., & Miki, H. (1978) *Chem. Pharm. Bull. 26*, 2449–2453.
IUPAC–IUB Commission on Biochemical Nomenclature (1970) *Biochemistry 9*, 4022–4027.
IUPAC–IUB Commission on Biochemical Nomenclature (1977) *Proc. Natl. Acad. Sci. U.S.A. 74*, 2222–2230.
Johnson, N. P., & Schleich, T. (1974) *Biochemistry 13*, 981–987.
Lee, C.-H., Ezra, F. S., Kondo, N. S., Sarma, R. H., & Danyluk, S. S. (1976) *Biochemistry 15*, 3627–3638.
Olsthoorn, C. S. M., Haasnoot, C. A. G., & Altona, C. (1980a) *Eur. J. Biochem. 106*, 85–95.
Olsthoorn, C. S. M., Bostelaar, L. J., van Boom, J. H., & Altona, C. (1980b) *Eur. J. Biochem. 112*, 95–110.
Quigley, G. J., Seeman, N. C., Wang, A. H.-J., Suddath, F. L., & Rich, A. (1975) *Nucleic Acids Res. 2*, 2329–2341.
Seeman, N. C., Rosenberg, J. M., Suddath, F. L., Kim, J. J. P., & Rich, A. (1976) *J. Mol. Biol. 104*, 109–144.
Uesugi, S., Miki, H., Ikehara, M., Iwahashi, H., & Kyogoku, Y. (1979) *Tetrahedron Lett.*, 4073–4076.
Uesugi, S., Takatsuka, Y., Ikehara, M., Cheng, D. M., Kan, L. S., & Ts'o, P. O. P. (1981a) *Biochemistry 20*, 3056–3062.
Uesugi, S., Shida, T., & Ikehara, M. (1981b) *Chem. Pharm. Bull. 29*, 3573–3585.
Warshaw, M. M., & Tinoco, I., Jr. (1965) *J. Mol. Biol. 13*, 54–64.
Warshaw, M. M., & Cantor, C. R. (1970) *Biopolymers 9*, 1079–1103.

Phosphorothioate Substrates for T4 RNA Ligase†

F. R. Bryant and S. J. Benkovic*

ABSTRACT: Stereochemical details of the T4 RNA ligase reaction mechanism have been delineated by examining the reactivity of phosphorothioate analogues in the adenosine 5′-triphosphate (ATP) dependent and ATP-independent RNA ligase reactions. Only the S_P isomer of the diastereomeric dinucleoside thiopyrophosphate, App(s)I, was active as an activated donor substrate in the ATP-independent RNA ligase reaction. The thiophosphodiester linkage in the ligation product, ApApAp(s)I, that is formed by the reaction of App(s)I (S_P) with the oligonucleotide acceptor, ApApA, was shown to have the R_P configuration. This indicates that phosphodiester bond formation occurs by a direct, nucleophilic displacement of AMP from App(s)I by the 3′-hydroxyl group of ApApA with inversion of configuration at phosphorus. The adenylylated intermediate, App(s)Ap, that is formed from the phosphorothioate donor, p(s)Ap, in the ATP-dependent RNA ligase reaction was shown to have the same stereochemical configuration as is required for the ATP-independent RNA ligase reaction. These results indicate that RNA ligase maintains a preferred chirality at phosphorus through the adenylylation and ligation steps of the reaction mechanism. An unusual result is the accumulation of adenosine cyclic 2′,3′-phosphate 5′-phosphorothioate in the ATP-dependent RNA ligase reaction employing the donor p(s)Ap when the acceptor ApApA is present. This observation suggests that there are two distinct but reactive modes for donor molecules.

RNA ligase from bacteriophage T4-infected *Escherichia coli* catalyzes the ATP-dependent formation of a 3′–5′ phosphodiester bond between the 3′-hydroxyl group of one oligoribonucleotide (the acceptor) and the 5′-phosphoryl group of a second oligoribonucleotide (the donor), thereby producing a covalently joined product. This reaction occurs via a minimal three-step mechanism outlined in Scheme I.

Scheme I

$$E + ATP \rightleftarrows E\text{–}pA + PP_i \quad (1)$$

$$E\text{–}pA + pN_n \rightleftarrows E[A\text{-}5'pp5'\text{-}N_n] \quad (2)$$

$$E[A\text{-}5'pp5'\text{-}N_n] + M_m \rightleftarrows M_mpN_n + AMP + E \quad (3)$$

$$n \geq 1 \qquad m \geq 3$$

† From the Department of Chemistry, The Pennsylvania State University, University Park, Pennsylvania 16802. *Received April 12, 1982.* This investigation was supported by a grant from the National Institutes of Health (GM13306).

0006-2960/82/0421-5877$01.25/0